Elastic transverse electron scattering form factors of ^{11}Li exotic nucleus

R. A.Radhi[1], Z. A. Dakhil[1], B. S. Hameed[2]

[1]Department of Physics, College of Science, University of Baghdad

[2]Department of Physics, College of Science for Women, University of Baghdad

E-mail: banalqazaz@yahoo.com

Abstract

The elastic transverse electron scattering form factors have been studied for the ^{11}Li nucleus using the Two- Frequency Shell Model (TFSM) approach. The single-particle wave functions of harmonic-oscillator (HO) potential are used with two different oscillator parameters b_{core} and b_{halo}. According to this model, the core nucleons of ^{9}Li nucleus are assumed to move in the model space of *spsdpf*. The outer halo (2-neutron) in ^{11}Li is assumed to move in the pure $1p_{1/2}$, $1d_{5/2}$, $2s_{1/2}$ orbit. The shell model calculations are carried out for core nucleons using the *spsdpf*-interaction. The elastic magnetic electron scattering of the stable ^{7}Li and exotic ^{11}Li nuclei are also investigated through Plane Wave Born Approximation (PWBA). It is found that the difference between the total form factors of unstable isotope (^{11}Li halo) and stable isotope ^{7}Li is in magnitude. The measured value of the magnetic moment is also reproduced.

Key words

Halo Nuclei, Exotic nuclei, Two-frequency shell model, Transverse electron scattering form factors, Magnetic moment.

Article info.

Received: Nov. 2013
Accepted: Feb. 2014
Published: Apr. 2014

عوامل التشكل المستعرضة للأستطارة الألكترونية المرنة للنواة الغريبة ^{11}Li

رعد عبد الكريم راضي[1]، زاهدة أحمد دخيل[1]، بان صباح حميد[2]

[1]قسم الفيزياء، كلية العلوم، جامعة بغداد

[2]قسم الفيزياء، كلية العلوم للبنات، جامعة بغداد

الخلاصة

تم دراسة عوامل التشكل المستعرضة للأستطارة الألكترونية المرنة لنواة ^{11}Li باستخدام أنموذج القشرة ذو الترددين. استخدمت الدوال الموجية للجسيمة المفردة لجهد المتذبذب التوافقي مع قيمتين مختلفتين للثابت التوافقي واحدة للقلب (b_{core}) والأخرى للهالة (b_{halo}). بناءاً على هذا الأنموذج، تم أفتراض نيكلونات القلب لنواة ^{9}Li تتحرك في فضاء *spsdpf*. تم أفتراض نيترونين الهالة لـ ^{11}Li بانها تسبح في المدارات الصرفة $1p_{1/2}$, $1d_{5/2}$, $2s_{1/2}$. تم تنفيذ وحساب أنموذج القشرة لنيكلونات القلب بأستخدام تفاعل *spsdpf*. كما تم تحقيق عوامل التشكل المغناطيسية للأستطارة الألكترونية المرنة للنواتين المستقرة ^{7}Li والغريبة ^{11}Li بواسطة تقريب بورن للموجة المستوية. لقد وجد هناك أختلاف لقيم عوامل التشكل المرنة للنواة الغريبة ^{11}Li والنواة المستقرة ^{7}Li. تم كذلك استنساخ القيم المقاسة للعزم المغناطيسي.

Introduction

Elastic electron scattering is a powerful technique for determining the ground-state charge and current distributions of nuclei. Coulomb electron scattering has been utilized to determine precise and detailed nuclear charge distributions, and magnetic electron scattering has provided information on nuclear current distributions. According to the shell model, nuclear magnetism is determined by valence nucleons. Therefore,

magnetic electron scattering gives insight into the single-particle aspects of the nucleus. Such scattering can arise from interactions with not only orbital currents but also spin currents, and so can be used to study the single-particle wave functions of both neutrons and protons.

The advantages of using electrons in the investigation of the nuclear structure are mainly related to the fact that the electron-nucleus interaction is relatively weak. For this reason multiple scattering effects are usually neglected and the scattering process is described in terms of perturbation theory. Since the reaction mechanism in perturbation theory is well under control the connection between the cross section and quantities such as charge distributions, transition densities, response functions etc., is well understood [1].

Until the middle of 1980's, nuclear physics had been developed by investigating primarily stable nuclei which exist in nature. Many facets of atomic nuclei had been revealed, which include a mass, density distribution, radius, shell structure, collective excitations, and various decay modes[2]. The field of halo nuclei has generated much excitement and many hundreds of papers since its discovery in the mid-1980s. While early β- and γ-decay studies of many of these nuclei yielded information about their lifetimes and certain features of their structure, credit for their discovery should go mostly to Tanihata [3,4] for the work of his group at Lawrence Berkeley Laboratory's Bevalac in 1985 on the measurement of the very large interaction cross sections of certain neutron-rich isotopes of helium and lithium, along with Hansen and Jonson for their pioneering paper two years later in which the term 'halo' was first applied to these nuclei [5]. The halo nuclei are an extreme case of exotic nuclei with almost zero binding energy.

The quadrupole and magnetic moment of exotic nuclei are serious tests for these new developed nuclear patterns. They contain a lot of information about the structure of the nuclear state: the magnetic dipole moment is sensitive to the orbitals of nucleons that are not dual to zero spin. The electric quadrupole moment shows information on the deformation of the charge distribution of the nucleus.

Suzuuki et al., [6] studied electric dipole (E1) and spin-dipole strength distribution of ^{11}Li by shell model calculations with halo effect. Two peaks in the E1 strength are found in the low excitation energy region below E_x=4MeV, which have almost the same energies as observed peaks in the Coulomb breakup reaction of ^{11}Li. The calculated E1 strength up to E_x=4MeV exhaust about 4% of the Thomas-Reiche-Kuhn energy –weighted sum rule value (The Thomas-Reiche-Kuhn (TRK) sum rule was discovered around the date of quantum mechanics founding). They found also pigmy and giant peaks in spin-dipole strengths of ^{11}Li. Possible existence of double soft dipole mode and giant resonance built on the soft dipole states are investigated.

Ren and Li [7] reviewed and discussed the three-body calculations on halo nuclei. It is concluded that the ground state properties of halo nuclei ^{11}Li, ^{14}Be and ^{17}B are independent of the shape of two-body potentials and an explanation on it is given. It is also shown that an introduction of a three-body interaction may be useful for a good explanation of the properties of halo nuclei.

Karataglidis and Amos [8] presented results for the elastic scattering of electrons and protons from the exotic He and Li isotopes. Comparison with scattering results from the stable He and Li nuclei allows for an investigation into the effects that the extensive neutron distributions have on the

charge density. For comparison, they also consider the proton halo nucleus ^{8}B. The consequences and possible suggestions for proposed electron scattering facilities for exotic nuclei are discussed. The same group [9] studied the elastic electron scattering form factors, longitudinal and transverse, from the He and Li isotopes and from ^{8}B. Large space shell model functions have been assumed. The precise distribution of the neutron excess has little effect on the form factors of the isotopes though there is a mass dependence in the charge densities. However, the form factors of the one proton halo nucleus, ^{8}B, are significantly changed by the presence of the proton halo.

Dong and Ren [10] investigated the effects of the velocity-dependent force on the magnetic form factors and magnetic moments of odd-Z nuclei. The form factors are calculated with the harmonic-oscillator wave functions. It is found that the contributions of the velocity-dependent force manifest themselves in the very large momentum transfer region ($q \geq 4$ fm^{-1}). In the low and medium q region the contributions of the velocity-dependent force are very small compared with those without this force. However, in the high-q region the contributions of the velocity-dependent force are larger than the normal form factors. The diffraction structures beyond the existing experimental data are found after the contributions of the velocity-dependent force are included. The formula of the correction to the single particle magnetic moment due to the velocity-dependent force is reproduced exactly in the long-wavelength limit (q = 0) of the M1 form factor.

The aim of the present work is to study of the transverse elastic electron scattering and calculate the magnetic dipole moments of exotic nucleus ^{11}Li (neutron-rich) using the Two- Frequency Shell Model (TFSM) approach. The shell model calculations are carried out for core nucleons using the *spsdpf*-interaction. The elastic magnetic electron scattering of the stable^{7}Li and exotic ^{11}Li nuclei are also investigated through Plane Wave Born Approximation (PWBA).

Theory

The interaction of the electron with the spin and currents distributions of the nuclei can be considered as an exchange of a virtual photon with angular momentum ± 1 along $\vec{q}$ direction. This is called transverse scattering [11]. From the parity and angular momentum selection rules, only electric multipoles can have longitudinal components, while both electric and magnetic multipoles can have transverse components [11, 12].

The squared form factors for electron scattering between nuclear states J_i and J_f involving angular momentum transfer J are given by [13]:

$$\left|F_J^{\eta}(q)\right|^2 = \frac{4\pi}{Z^2(2J_i+1)} \times \left| \sum_{T=0,1} (-1)^{T_f - T_{zf}} \begin{pmatrix} T_f & T & T_i \\ -T_{Zf} & M_T & T_{Zi} \end{pmatrix} \left\langle \Gamma_f \left\| \hat{T}^{\eta}_{J,T}(q) \right\| \Gamma_i \right\rangle \right|^2 \quad (1)$$

the superscript η represents longitudinal (L) or transverse (T) electric (E) and magnetic (M), $\hat{T}_J^{\eta}(q)$ is the electron scattering multipole operator.

The squared transverse form factors are given [13] as the sum of the squared electric form factor and squared magnetic form factor as follows:

$$\left|F_J^{T}(q)\right|^2 = \left|F_J^{E}(q)\right|^2 + \left|F_J^{M}(q)\right|^2 \quad (2)$$

For a selected operator T^{η}_{JT} the reduced matrix elements are written as the sum of the product of the one-body density matrix elements (OBDM) times the single-particle transition matrix elements [14]:

$$\left\langle \Gamma_f \left\| \hat{T}^{\eta}_{\Lambda} \right\| \Gamma_i \right\rangle = \sum_{\alpha,\beta} OBDM\left(\Gamma_i,\Gamma_f,\alpha,\beta\right) \left\langle \alpha \left\| \hat{T}^{\eta}_{\Lambda} \right\| \beta \right\rangle \quad (3)$$

where $\Lambda = JT$ is the multipolarity and the states $\Gamma_i \equiv J_i T_i$ and $\Gamma_f \equiv J_f T_f$ are initial and final states of the nucleus. While α and β denote the final and initial single-particle states, respectively (isospin is included).

The single-nucleon form factor [15] and the center-of-mass form factor [16] are given by:

$$F_{fs}(q) = [1+(q/4.33)^2]^{-2},\ F_{cm}(q) = e^{q^2 b^2/4A} \quad (4)$$

where A is the nuclear mass number and b is the harmonic-oscillator size parameter, for halo nuclei b equal to the average of b_{core} and b_{halo}. Introducing these corrections into Eq (1), we obtain:

$$\left|F^{\eta}_{J}(q)\right|^2 = \frac{4\pi}{Z^2(2J_i+1)} \times \left| \sum_{T=0,1} (-1)^{T_f - T_{zf}} \begin{pmatrix} T_f & T & T_i \\ -T_{Zf} & M_T & T_{Zi} \end{pmatrix} \left\langle \Gamma_f \left\| \hat{T}^{\eta}_{J,T}(q) \right\| \Gamma_i \right\rangle \right|^2 \times \left|F_{c.m}(q)\right|^2 \times \left|F_{f.s}(q)\right|^2 \quad (5)$$

The electromagnetic moments $m(\lambda J)$ through 3j-symbol [17, 18];

$$m(\lambda J) = \left[\frac{4\pi}{2J+1}\right]^{\frac{1}{2}} \begin{pmatrix} J_i & J & J_i \\ -J & 0 & J_i \end{pmatrix} M(\lambda J) \quad (6)$$

where $M(\lambda J)$ is the γ-decay transition matrix elements and is given by;

$$M(\lambda J) = \underset{q \to E_x/\hbar c}{Lim} \frac{(2J_i+1)^{1/2}(2J+1)!!\, Z\,[J/(J+1)]^{1/2}}{q^L \sqrt{4\pi}} F^{mag}_{T}(J,q) \quad (7)$$

Results and Discussion

The shell model has been successful in reproducing the magnetic moments by the spin and orbital *g*-factors for free nucleons. The differences between the single particle *g*-factors and the measured values have been explained by the configuration mixing: the core nucleus composed of an even number of nucleons is excited into the 1^+ state, which contributes to the magnetic moment of the nucleus.

According to the many – particle shell model, the stable nucleus ^{7}Li is considered as a core of ^{4}He plus three nucleons distributed over the $1p_{3/2}$ and $1p_{1/2}$ orbits. The single – particle wave functions of harmonic oscillator potential with size parameter b_{rms}=1.74fm chosen to reproduce the root mean square charge radius. Fig. 1 represents the transverse form factors of ^{7}Li ground state ($J^{\pi} T = \frac{3^-}{2}\ \frac{1}{2}$) for the *spsdpf*-model space with the size parameter b_{rms}=1.74fm (solid curve). The results are compared with the experimental data of Niftrik et al.[19] (squares) and with the data of Lichtenstadt et al .[20] (circles). The individual multipoles contributions M1 and M3 are denoted by dashed and dashed-dot curves respectively, while the E2 multipole is disappeared because it has a negligible contribution. The M1 and M3 multipoles can be easily distinguished, since they peak at different locations of q (around 0.5 and 2.1 fm^{-1} respectively). The M3 multipole is dominant over the diffraction minimum of M1 multipole. The experimental data are very well reproduced at low momentum transverse (q $<$1.0) in 1*p*–shell model space (solid curve), but they are overestimated at high q–value.

The calculated magnetic dipole moment $\mu = 3.165 n.m$ is in an excellent agreement with the measured value $\mu_{\exp.} = 3.256 n.m$ [21].

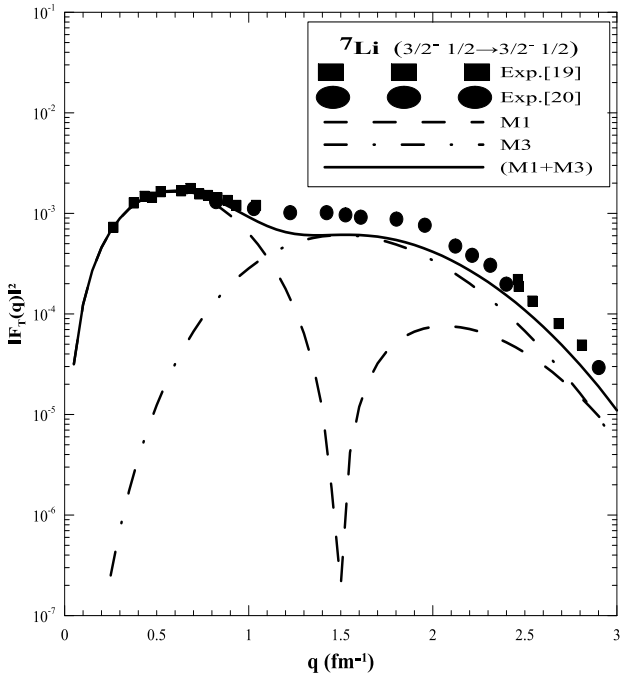

Fig. 1: The transverse form factors for ^{7}Li ground state calculated in spsdpf model space. The individual multipole contribution of M1 and M3 are shown. The data are taken from Ref. [19] (square) and Ref. [20] (circles).

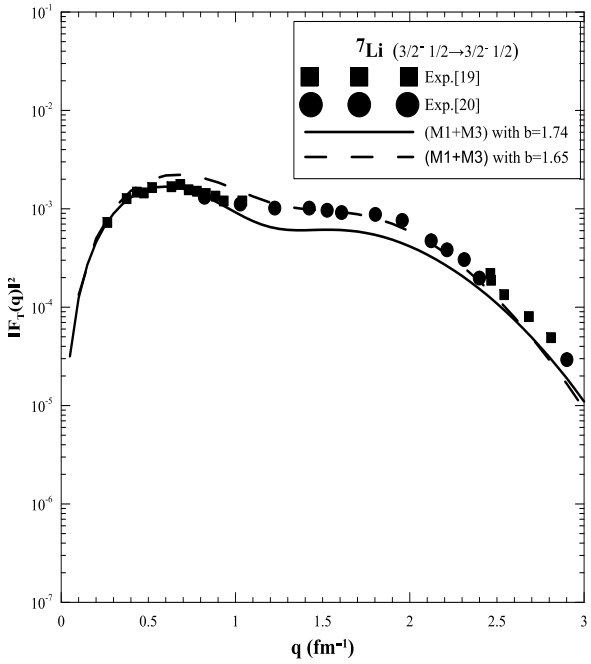

Fig. 2: Comparison between the total form factors of ^{7}Li nucleus with the size parameter b=1.74fm (solid curve). and b=1.65fm (dashed curve).

The results are improved if the size parameter of the harmonic oscillator potential reduced from that required to reproduce the rms by 5% (b=1.65fm) as shown by the dashed curve in Fig. 2. The experimental data are very well reproduced at $1.4 \leq q \leq 2.4$ fm^{-1}.

The form factors of unstable nucleus ^{11}Li (non-halo) with $J^\pi T = 3/2^-\ 5/2$ is calculated for the *spsdpf*-model space with size parameter b_{rms}=2.22 fm chosen to reproduce the root mean square charge radius 3.12±0.16 [22] as shown in Fig. 3. The calculated form factors of isotope nucleus ^{11}Li are compared with the experimental data of stable ^{7}Li nucleus (solid curve) .The diffraction minimum located at momentum transfer q=1.2 fm^{-1} and the diffraction maximum located at q=0.5 and 1.55 fm^{-1}. The individual multipoles contributions M1 and M3 are denoted by dashed and dashed-dot curves respectively.

The microscopic structure of unstable nucleus ^{11}Li with $J^\pi T = 3/2^-\ 5/2$ ($\tau_{1/2}$=8.8 ms [23]) is imagined as being composed of a tightly bound core ^{9}Li with $J^\pi T = 3/2^-\ 3/2$ ($\tau_{1/2}$=178.3 ms [24]) plus two loosely bound neutrons ($J^\pi T = 0^+1$) (two neutrons halo is called Borromean [25],since none of the binary subsystems of the core plus two nucleon are founded in bound state). In the present work, the same model spaces are chosen for the core and the extra two neutrons. The configurations $(1s_{1/2})^4$, $(1p_{3/2})^5$ are used for ^{9}Li and with the configuration $1p_{1/2}$,$1d_{5/2}$, $2s_{1/2}$ are used for the two neutron halo. To obtain the OBDMs, the nuclear shell model calculation is performed in the mentioned space using the *spsdf* interaction.

The form factors of unstable nucleus ^{11}Li (halo) with $J^\pi T = 3/2^-\ 5/2$ is calculated for the *spsdpf*-model space with the value of the oscillator size parameter b_{core}=1.62 fm is chosen for ^{9}Li, which gives the rms radius equal to 2.32 fm, that is in agreement with

the measured value 2.32±0.02 [22], and b_{halo}=3.6 fm is chosen for two neutron halo as shown in Fig. 4. The diffraction minimum located at momentum transfer q=1.6 fm^{-1} and the diffraction maximum located at at q=0.6 and 2.2 fm^{-1}. The location of the minimum of ^{11}Li (halo) has outward shifted as compared with the minimum of ^{11}Li (non-halo). The calculated magnetic moment $\mu = 3.792\, n.m$ is an excellent agreement with the measured value $\mu_{exp.} = 3.6678\, n.m$ [26].

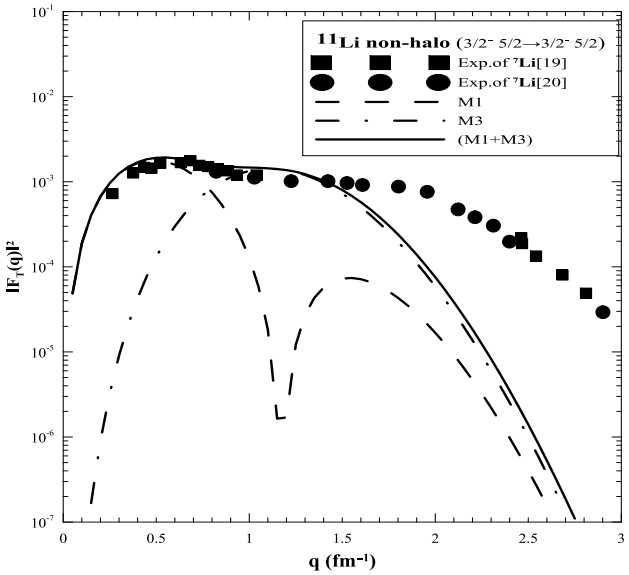

Fig. 3: The transverse form factors for ^{11}Li (non-halo) ground state calculated in spsdpf model space. The individual multipole contribution of M1 and M3 are shown. The data are the same as in Fig. 1.

Fig. 5 represents comparison of the total form factors of ^{11}Li (halo) (solid curve) and the calculated form factors of ^{11}Li (non-halo) (dashed curve) with the experimental data of ^{7}Li nucleus. The total form factors of ^{11}Li (halo) have the same shape as the calculated form factors of ^{11}Li (non-halo) but they are different in magnitude.

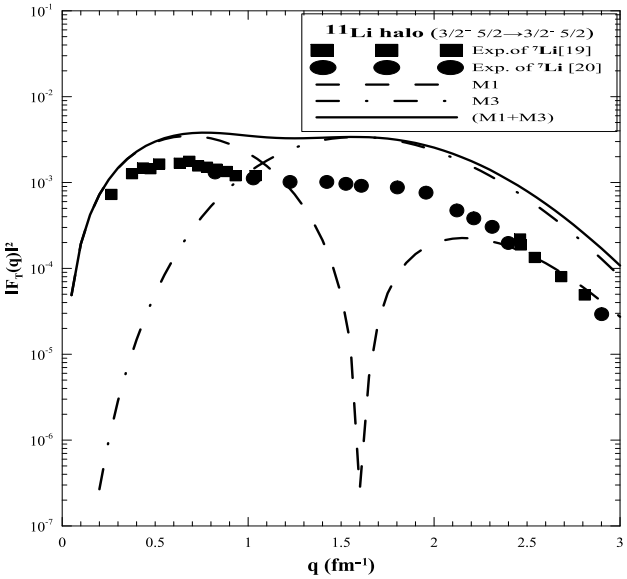

Fig. 4: The transverse form factors for ^{11}Li (halo) ground state calculated in spsdpf model space. The individual multipole contribution of M1 and M3 are shown. The data are the same as in Fig. 1.

Comparison between the total form factors of ^{11}Li (halo) (solid curve), ^{9}Li (dot-dashed curve) and ^{7}Li (dashed curve) with the experimental data of ^{7}Li nucleus as shown in Fig. 6. The total form factors of ^{11}Li (halo) have the same behaviors as the calculated form factors of ^{9}Li and ^{7}Li but they are different in magnitude. The form factor is not dependent on detailed properties of the neutron halo. The difference between the total form factors of ^{11}Li (halo),^{9}Li and ^{7}Li is due to the different center of mass correction of these nuclei. The difference between the center of mass correction of ^{11}Li (halo),^{9}Li and ^{7}Li is essentially due to the difference of the mass number and the size parameter b which is assumed in this case equal to the average of b_{core} and b_{halo} and the difference is attributed to the difference in the recoil effect.

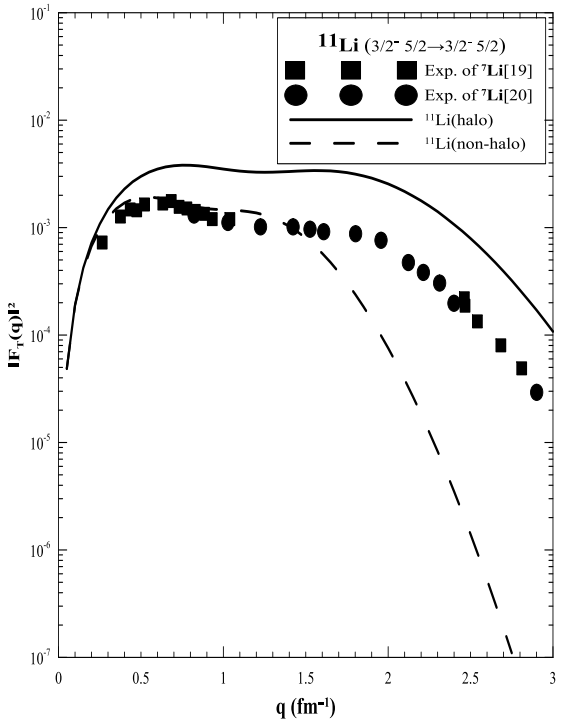

Fig. 5: Comparison between the total form factors of ^{11}Li (non-halo) (dashed curve) and ^{11}Li (halo) (solid curve) with the experimental data of ^{7}Li nucieus.

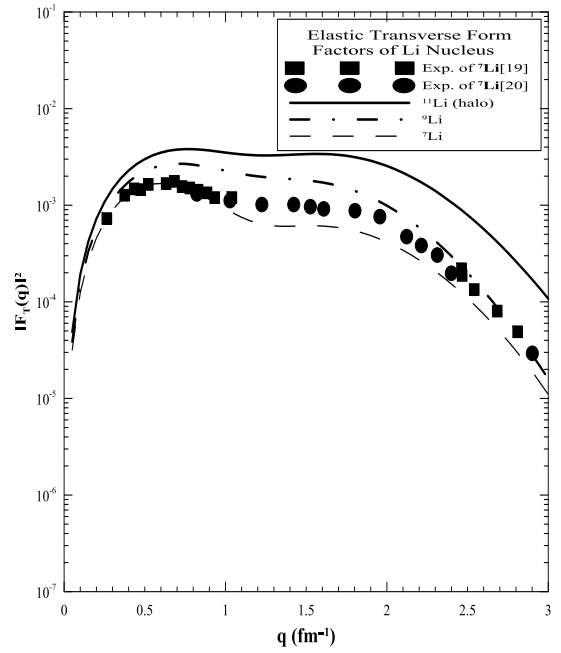

Fig. 6: Comparison between the total form factors of ^{11}Li (halo) (solid curve), ^{9}Li (dot-dashed curve) and ^{7}Li (dashed curve) with the experimental data of ^{7}Li nucleus.

Conclusion

In the present work, it is possible to draw the following conclusions:

1. The total form factors of ^{11}Li (halo) have the same behavior as the calculated form factors of ^{9}Li and ^{7}Li but they are different in magnitude.
2. For neutron-halo nuclei, it is found that the form factors are not dependent on detailed properties of the neutron halo. The only difference between form factors of the unstable nucleus and that of stable is attributed to the difference in the center of mass correction.
3. The calculated elastic form factors for neutron-rich nuclei ^{11}Li (halo) showed a forward shifts in comparison with ^{11}Li (non-halo) and with stable one (^{7}Li).
4. With the use of Two- Frequency Shell Model (TFSM) approach, the calculated magnetic moment is an excellent agreement with the measured value.

References

[1] R. Hofstadter, Rev. Mod. Phys., 28 (1956) 214.
[2] K. Hagino, I. Tanihata, H. Sagawa, Nucl. Exp. ,1208.1583v2 [nucl-th] 14 Aug (2012).
[3] I. Tanihata, H. Hamagaki, O. Hashimoto, Y. Shida, N. oshikawa, K. Sugimoto, O.Yamakawa, T. Kobayashi, and N. Takahashi, hys. Rev. Lett., 55 (1985) 2676.
[4] I. Tanihata, H. Hamagaki, O. Hashimoto, S. Nagamiya, Y. Shida, N. Yoshikawa, O. Yamakawa, K. Sugimoto, T.Kobayashi, D.E. reiner, N. Takahashi, Y. Nojiri, Phys. Lett., B160 (1985) 380.
[5] J. Al-Khalili, Lect. Notes Phys., 651 (2004) 77–112.
[6] T. Suzuki, H. Sagawa, P.F. Bortignon, Nucl. Phys., A 662 (2000) 282-294.
[7] Z. Ren and N. Li, Mod. Phys. Lett., A, 18, 2-6 (2003) 174-177.
[8] S. Karataglidis and K. Amos, Ric. Sci. Educ. Perm., Suppl., 126, nucl-th/0607010v (2006).

[9] S. Karataglidis and K. Amos, Phys. Lett. B, 650 (2007) 148-151.
[10] T. Dong, Z. Ren, Chin.Phys.Lett., 253 (2008) 884.
[11] T. de Forest and J.D Walecka, Adv. Phys. ,15 (1966) 1.
[12] T.de Shalit and I.Talmi " Nuclear Shell Theory ", Acadimic New York, 1963.
[13] T. W. Donnelly and I. Sick, Rev.Mod. Phys. 56 (1984) 461.
[14] P.J. Brussaard and P. W. M. Glademans, "Shell-model Application in Nuclear Spectroscopy", North-Holland Publishing Company, Amsterdam (1977).
[15] J. P. Glickman, W. Bertozzi, T. N. Buti, S. Dixit, F. W. Hersman, C. E. Hyde-Wright, M. V. Hynes, R. W. Lourie, B. E. Norum, J. J. Kelly, B. L. Berman, and D. J. Millener, Phys. Rev., C43 (1991) 1740.
[16] T. Tassie and F. C. Barker, Phys. Rev., 111 (1958) 940.
[17] R. A. Radhi, Ph.D.Thesis, Michigan state University, USA, (1983).
[18] B.A. Brown, B.H. Wildenthal, C.F. Williamson, F.N. Rad, S. Kowalski, H. Crannell and J.T. O'Brien, Phys. Rev. C32, 4(1985) 1127.
[19] G. Van Niftrik , L.Lapikas, H.Devries and G.Box, Nucl. Phys. A174 (1971) 173.
[20] J. Lichtenstadt, J. Alster, M. A. Moinester, J. Dubach, G .A .Peteson and S. Kowaski , Phys.Lett, 121 B, 6, (1983) 377
[21] F.Ajezenberg- Selove, Nucl. Phys., A490 (1988) 1.
[22] I. Tanihata, T. Kobayashi, O. Yamakawa, S. Shimoura, K. Ekuni, K. Sugimoto, N.Takahashi, T. Shimoda, and H. Sato, Phys. Lett B, 206 (1988) 592
[23] A. S. Jensen, K. Riisager, D. V. Fedorov and E. Garrido, Rev. Mod. Phys., 76 (2004) 215.
[24] Radioactive Nuclear Beam Facilities, NuPECC Report , Europe, (2000).
[25] M. Zukov, B. Danilin, D. Fedorov, J. Bang, I. Thompson and J.Vagen, Phys. Rep.,231 (1993) 151.
[26] P.Raghavan, Atomic Data and Nuclear Data Tables, 42 (1989) 189.